

LONG-RANGE EARTHQUAKE FAULT MODELS

**Charles D. Ferguson, W. Klein,
and John B. Rundle**

Department Editors: Harvey Gould

hgould@clarku.edu

Jan Tobochnik

jant@kzoo.edu

[S0894-1866(98)00501-X]

Understanding the physics of complex phenomena such as earthquakes is a formidable challenge. Because we are constrained by our inability to do experiments on earthquake faults, we turn to computers as our earthquake laboratories. Computer simulations of earthquakes help us to test theoretical models and allow us to generate catalogs of synthetic earthquake events. In this column, we discuss several models and algorithms for simulating strike-slip faults with nearest-neighbor and long-range interactions.

We begin by briefly reviewing the essential physics of earthquakes (see Ref. 1 for a more complete introduction and Ref. 2 for a more advanced exposition). A strike-slip or transform fault, such as the San Andreas fault in California, delineates the boundary between two crustal regions that move primarily along the earth's surface and opposite to each other. Although earthquakes occur at other types of faults, we shall concentrate solely on strike-slip earthquakes, which have their initial rupture sites near the earth's surface, because their mainly one-dimensional motion makes them easier to simulate than other types of faults.

Without the earth's relatively rigid upper layer, called the lithosphere, these shallow-focus quakes would not occur. The lithosphere, an approximately 100-km-thick layer, which is made of the crust and a portion of the upper mantle, consists of two principal parts that are coupled. Although the upper part can sustain tremendous shear

stresses (about 10 MPa in faults and about 100 MPa in the surrounding rock) and undergoes brittle fracture and seismic slip, the lower part behaves ductilely and experiences aseismic slip. Seismic slip is associated with earthquakes and refers to very rapid motion due to a frictional instability between the two sides of a fault. After undergoing seismic slip, the formerly sliding rock experiences an interval of little or no motion during which the stress on the rock recharges. This phenomenon is called a stick-slip instability. In contrast, aseismic slip refers to continuous, usually slow, stable sliding and is not associated with earthquakes. Consequently, the lower part constrains earthquakes to the upper region of the lithosphere and prevents large earthquakes from expanding to below the border between the upper and lower regions. This constraint may lead to differences in the distribution of occurrence frequency versus size for large and small earthquakes.³

What do geophysical theories tell us about strike-slip earthquakes? The theory of plate tectonics says that the lithosphere is broken into about a dozen major rigid plates and several minor ones. These plates slowly grind against each other, building up stress and creating faults. The elastic rebound theory,⁴ the first modern theory of earthquakes, emphasizes the importance of elastic strain energy in earthquake generation and states that the elastic strain increases monotonically on a fault, a previously weakened region, resulting in an increase of stress. Once the stress accumulates to the breaking strength, this region becomes unstable and rapidly rebounds or slips to a lower, more stable stress state. The released elastic strain energy manifests itself as seismic radiation and violent ground motion and rearrangement. After the earthquake subsides, tectonic forces renew the gradual buildup of stress on the fault, eventually culminating in another earthquake.

Seismologists have observed that small quakes occur

Charles D. Ferguson is a postdoctoral research associate at the Institute for Physical Science and Technology, University of Maryland, College Park, MD 20742; W. Klein is a professor of physics at the Department of Physics, Center for Polymer Physics, and Center for Computational Science, Boston University, Boston, MA 02215; John B. Rundle is a professor of geology and physics at the Department of Geological Sciences, Department of Physics, and Cooperative Institute for Research in Environmental Sciences, University of Colorado, Boulder, CO 80309 and is the director of the Colorado Center for Chaos and Complexity.

more frequently than large quakes. Gutenberg and Richter⁵ established a scaling relation between the magnitude m and frequency of occurrence of earthquakes. For our purposes, we take $m \propto \log_{10} A$, where A is the rupture area and a measure of the size of an earthquake (see Ref. 1 for the definition of the Richter magnitude). The Gutenberg and Richter scaling relation is

$$\log_{10} N(m) = a - bm, \quad (1)$$

where a and b are constants and $N(m)$ is the number of earthquakes greater than m in a specified time interval. Although the form of the relation (1) is universal, the values of a and b depend on the region. The constant a specifies a region's level of seismicity, that is, the activity, where a large a implies a high level of regional seismicity. The values of b are generally between 0.75 and 1.5, where smaller b values indicate more quakes within a given time interval. Large earthquakes ($m > 7$) have different values of b ($1.2 < b < 1.5$) than small quakes ($0.75 < b < 1.2$).³ This difference in the scaling-relation coefficients in the two cases may be a result of the exclusion of large earthquakes from the ductile region of the lithosphere as described above.

The form of Eq. (1) implies a power-law relation, $N \sim A^{-b}$. This relation has motivated physicists to ask if this and other power-law relations for additional properties of earthquakes imply a kind of critical phenomenon. In other words, are earthquakes a kind of phase transition? A first check on the robustness of an earthquake-fault model is that it be able to produce these scaling relations. However, the ability to produce a scaling relation does not mean that the model is useful, because it also must be able to reproduce other known phenomena and lead to predictions that seismologists can observe on real faults. Hopefully, by analyzing the successful models, we can answer this question about critical phenomena and come to a better theoretical understanding about earthquakes.

Now that we have covered some of the basic information about strike-slip faults, we discuss how to model them. In 1967, Burridge and Knopoff⁶ developed the first computer model of a fault. The Burridge and Knopoff (BK) model consists of a one-dimensional chain of massive slider blocks, where each block contacts a frictional surface (one side of the fault) and interacts with its nearest neighbors and a tectonic loader plate (the other side of the fault) via Hooke's law springs with spring constants K_C and K_L , respectively (see Fig. 1). The springs simplify the dynamics by restricting the blocks to move along or opposite to the plate's motion. As the loader plate slowly moves, it causes the force to increase linearly on each block to the point where the force equals the frictional failure threshold (the fault's breaking strength), after which the block slides to a lower residual force state. To produce a dynamic instability, BK chose a velocity-dependent frictional force that decreases as the sliding block's velocity increases.

The dynamics of the BK model is found using Newton's second law. The equation of motion for block i is

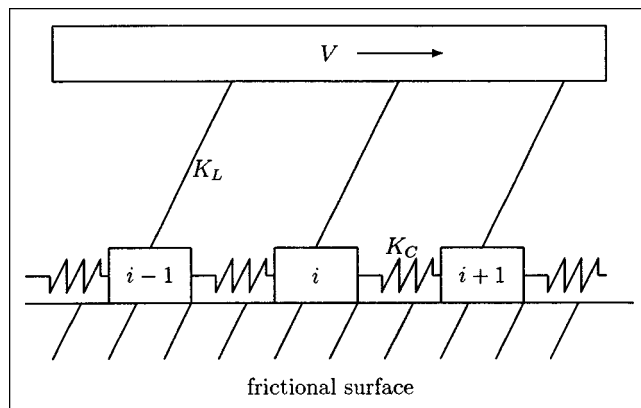


Figure 1. Schematic of the Burridge-Knopoff model.

$$m_i \ddot{x}_i(t) = K_C [x_{i+1}(t) - 2x_i(t) + x_{i-1}(t)] + K_L [Vt - x_i(t)] + F[\dot{x}_i(t)], \quad (2)$$

where $x_i(t)$ is the displacement of block i from its equilibrium position, m_i is the mass of block i , and V is the velocity of the loader plate. The function $F[\dot{x}_i(t)]$ embodies the velocity-weakening friction force and can include additional dissipative terms proportional to the velocity of block i as well as losses due to seismic waves, which are elastic waves that carry away some of the earthquake's energy.

A sliding block transfers force to its nearest neighbors as we can see by examining the first term on the right-hand side of Eq. (2), which couples block i to its nearest neighbors. If these neighbors receive enough additional force to cause them to slip, they can cause their neighbors to slip and so on, thereby generating a chain reaction of failure or an earthquake that stops once all blocks are below the failure threshold. Here and from now on, slip refers to seismic slip, as previously defined. Because the geophysical literature predominantly uses the term stress instead of force when discussing faults, we assume each block has the same unit area; henceforth, we will use stress rather than force.

For a large number of blocks ($N > 10^3$), the BK model is computationally time-consuming because it requires the solution of N coupled second-order ordinary differential equations of motion. Although it is possible to simulate the BK model and others similar to it (see, for example, Ref. 7), we will adopt a less computationally demanding approach that allows us to include more blocks and to compute for longer time intervals, resulting in improved statistics. Our model, based on work by Rundle, Jackson, and Brown (RJB),⁸ is a cellular-automaton version of the BK model and resembles the Olami, Feder, and Christensen model.⁹ The RJB model bypasses the need for differential equations, assigns each block to a cell on a lattice, and specifies a rule for how each cell interacts with its neighboring cells. Like the BK model, each block is connected to its nearest neighbors and a loader plate via linear springs, which restrict

each block's motion. Each block rests on a frictional surface and does not move unless its stress exceeds a static failure threshold σ_F .

Unlike the BK model, the RJB model simplifies the dynamics by using noninertial massless blocks, thus preventing the simulation of seismic waves. This approximation is appropriate as long as the friction and spring forces are much bigger than the inertial force (that is, the product of the mass and the acceleration). Faults typically exhibit a low seismic efficiency, that is, the fraction of strain energy converted to seismic waves is on the order of 5%–10%.¹⁰ For this reason, internal energy and entropic effects dominate inertial effects.¹¹ In addition, the exclusion of seismic radiation should not appreciably affect the statistical distribution of earthquakes. In support of this claim, Nakanishi¹² has shown that massless cellular-automata models can give the same quantitative results as massive slider-block models.

We first describe an algorithm for the nearest-neighbor RJB model and later modify it to include long-range interactions. We can either choose the reference frame of the frictional surface and measure the displacement $U_i(t)$ of block i from its initial position with respect to the frictional surface or choose the moving coordinate system of the loader plate. Because we want to know how far each block lags behind the plate, we select the second option and define the slip deficit as

$$\phi_i(t) = U_i(t) - nV\Delta T, \quad (3)$$

where V is the velocity of the loader plate and n is the number of loader-plate updates. The tectonic-force-transmission time scale, ΔT , is on the order of years because of the usually long time between earthquakes. In contrast, the other time scale of interest, the duration of an earthquake, can last from a few seconds to a few minutes, but typically is less than 30 s. Below we use the rupture time t to measure this duration. The algorithm for the nearest-neighbor RJB model can be summarized as follows:

(1) Assign either a uniform static failure threshold, where each block i has the same $\sigma_{F,i}$, or a random failure threshold, where $\sigma_{F,i}$ varies for each block and has the form $\sigma_{F,i} = \bar{\sigma}_F + (2\delta_i - 1)\sigma_A$; δ_i is a uniform random number $\in [0,1]$ and $\bar{\sigma}_F$ is the mean failure threshold. It is recommended that $\sigma_A \leq 0.2\bar{\sigma}_F$. Additionally, assign a residual stress $\sigma_{R,i}$ to each block i . The quantity $\sigma_{R,i}$ represents the stress on block i after it slips (see step 3). We usually set $\sigma_{R,i} = 0$. Also assign an initial slip deficit $\phi_i(0) \in [-\bar{\sigma}_F/K_L, 0]$ from a random uniform distribution to each block i , where K_L is the loader-plate spring constant. Set $n = 1$ and $t = 1$.

(2) Compute the total stress $\sigma_i(t)$ on each block i by

$$\sigma_i(t) = -K_L\phi_i(t) + K_C \sum_{j \in \text{nn}} [\phi_j(t) - \phi_i(t)], \quad (4)$$

where K_C is the spring constant between the blocks, and the sum includes only the nearest-neighbor (nn) blocks of block i .

(3) A block with $\sigma_i(t) > \sigma_{F,i}$ slips to its residual stress state $\sigma_{R,i}$ by applying

$$\phi_i(t+1) = \phi_i(t) + J[\sigma_i(t)]\Theta[\sigma_i(t) - \sigma_{F,i}], \quad (5)$$

where the step function $\Theta[x] = 1$ for $x > 0$ and $\Theta[x] = 0$ for $x \leq 0$. The jump function, $J[\sigma_i(t)]$, can be either deterministic

$$J[\sigma_i(t)] = J_d \equiv \frac{\sigma_i(t) - \sigma_{R,i}}{K}, \quad (6)$$

or stochastic

$$J[\sigma_i(t)] = J_s \equiv J_d(1 - \rho W). \quad (7)$$

The noise amplitude W is in the range $0 \leq W \leq 1$; ρ is a random number uniformly distributed in the interval $[0,1]$. The constant $K = K_L + qK_C$, where q is the number of neighboring blocks; $q = 4$ for nearest-neighbor interactions on a two-dimensional lattice. Block i dissipates JK_L units of stress. Increment the rupture time $t \rightarrow t + 1$.

(4) Repeat steps (2) and (3) until all $\sigma_i(t) < \sigma_{F,i}$.

(5) Measure the physical quantities of interest (see below).

(6) Move the plate a distance $V\Delta T$ by decreasing ϕ_i by $V\Delta T$ [see Eq. (3)], where $\Delta T = 1$, that is, each block receives $K_L V$ units of stress. Increment the loader-plate time $n \rightarrow n + 1$. Set $t = 1$.

(7) Return to step (2) and continue this procedure for a predetermined number of times.

We take the boundary conditions to be either periodic or closed. For periodic boundary conditions, the springs of the boundary blocks are connected to blocks on the opposite boundary, and hence stress cannot be dissipated through the boundaries, except via the loader plate. Each block has as many neighbors as every other block. Although these conditions could result in phase locking in which the same patterns or earthquakes repeat periodically, an unrealistic condition for earthquakes, adding noise by using the stochastic jump function prevents this behavior. For closed boundary conditions, the boundaries are isolated, and boundary blocks are not connected to blocks beyond the boundaries. Hence, these blocks have fewer neighbors so that the value of K for boundary blocks is less than the value of K for interior blocks. Accordingly, boundary blocks typically have greater jump-function values than interior blocks [see Eq. (6)], leading to more stress dissipation through the boundaries.

The identification of the blocks that are at or near failure can be computationally expensive, especially if we employ the zero-velocity-limit method for which $V \rightarrow 0$. In this method, the loader plate quasistatically loads stress into the system so that a single failing block, called the initiator, initiates an earthquake. This method ensures a clear separation between the time scale of years (n) for the tectonic

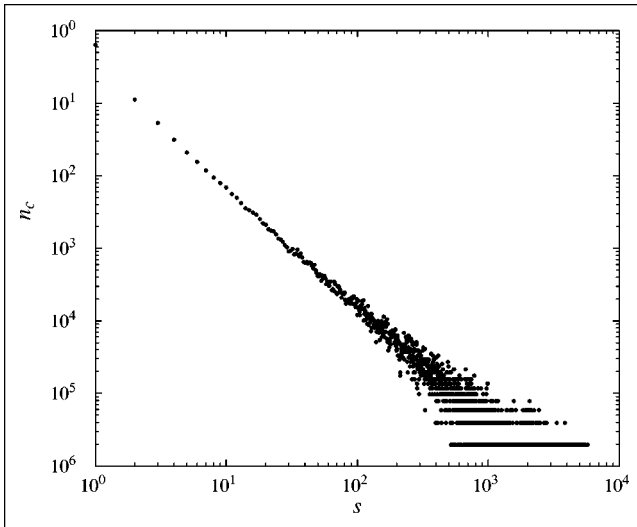


Figure 2. Log-log plot of the mean number of clusters $n_c(s)$ with s failed blocks for $L=128$, nearest-neighbor interactions, and closed boundary conditions. The parameters are $\sigma_F=50$, $\sigma_R=0$, $K_C=K_L=1$, and the zero-velocity-limit with the deterministic jump function. The negative of the slope corresponds to a cluster scaling exponent $\tau=1.6$ over the interval $1 \leq s \leq 300$, where $n_c(s) \sim s^{-\tau}$, implying that $b=0.9$.

(loader) plate and the time scale of seconds (t) for the earthquake rupture. Because we cannot run our simulations for years, we can shorten the process significantly by locating the block nearest to failure at the start of a loader-plate update and then moving the loader plate just enough to cause only that block to fail. The search for the initiator block requires typically $O(N)$ number of computations. However, by using a linked-list data structure, we can decrease this search to $O(1)$.¹³ An alternative to the zero-velocity-limit method is to choose a small constant $V \approx \bar{\sigma}_F/L^2$, which produces on average a single initiator per plate update.

Before making measurements, we need to let the system run for a sufficient number of plate updates [$O(10^4)$] so that each block has failed several times. This time will allow transients due to the initial conditions to disappear and will permit the system to reach a stationary state. During the simulation, quantities of interest include the size of an earthquake (the total number of failed sites per loader-plate update), the total rupture time per plate update, and the average system stress or slip deficit. We refer to the set of failed sites as a cluster.

In Fig. 2 we observe that the occurrence frequency of the clusters, $n_c(s)$, scales with cluster size s as $n_c(s) \sim s^{-\tau}$. As an encouraging check on the model, the power-law exponent $\tau=1.6$ is consistent with a Gutenberg-Richter value of $b \approx 1$, according to the relation $\tau=1+2b/3$ (see Ref. 14 for a derivation). The exponents b and τ are not equal because of a factor of $2/3$ difference between the Richter magnitude and our definition of the size of an earthquake and the fact that $N(m)$ in Eq. (1) is an integrated quantity,

whereas $n_c(s)$ is not.^{11,14} We describe other interesting measurements in the suggestions for further study.

Extending the nearest-neighbor RJB model is interesting for several reasons. Linear elasticity theory yields long-range stress tensors for a number of geophysical applications. In particular, for a dislocation in a three-dimensional homogeneous elastic medium, the static stress tensor $T \sim r^{-3}$,¹⁵ where r is the distance between the center of the dislocation and another point in the medium. Although geophysicists do not know the actual stress tensors for real faults, they expect that long-range stress tensors apply. Recently, Hill *et al.*¹⁶ have proposed models with both static r^{-3} and dynamic $r^{-3/2}$ stress tensors to explain why several earthquakes occurred within a few minutes after and as distant as 1200 km from the major 1992 Landers, California, earthquake. These stress tensors introduce long-range interactions between the Landers quake and the subsequent activity. It is suspected, but not yet investigated carefully, that microcracks in fault gouge, which is weak pulverized rock that has turned to clay, screen long-range interactions, resulting in a proposed $T \sim e^{-\alpha r}/r^3$ interaction, where $\alpha \ll 0.01 \text{ km}^{-1}$.¹⁷ This screening is important because strike-slip fault zones typically contain much fault gouge.

In the RJB model, a slider-block approximates a macroscopic fault asperity, a rough region on a fault surface, of the order of 100 m^2 . The interaction range varies and extends over a geological fault's depth on the order of 1 km^2 or more. Therefore, the model's interaction region must include on the order of 10^4 slider blocks to simulate this depth effect. On geological faults, the stress drop $\Delta\sigma$ due to an earthquake is about $0.01\text{--}1 \text{ MPa}$, and the failure stress σ_F is about 10 MPa .² Thus, the ratio $\Delta\sigma/\sigma_F$ is $0.001\text{--}0.1$. In the RJB model for constant σ_F , $\Delta\sigma/\sigma_F$ decreases to values consistent with geological values as the interaction range increases.¹¹ Consequently, the RJB model requires long-range interactions.

We know from studies of other long-range systems (such as long-range Ising models¹⁸) that long-range systems can exhibit different behavior than short-range systems. In fact, we find different statistical distributions in the RJB model using long-range interactions. The long-range RJB model has more neighbors and a different functional form of the interaction compared to the nearest-neighbor model. To convert the nearest-neighbor algorithm to a long-range algorithm, we make the following changes: In Eq. (4), the sum now includes blocks within a square neighborhood of area $(2R+1)^2$ centered about block i . For periodic boundary conditions, block i has $q=(2R+1)^2-1$ neighbors. For closed boundary conditions, block i has $q=(2R+1)^2-1$ neighbors if the position of i is greater than R units from a boundary and fewer neighbors if this position is less than R units from a boundary. We also introduce a distance-dependent stress tensor acting between neighbors that approximates the long-range interactions discussed above.

We consider two forms of the stress tensor: (a) \tilde{K}_C/r^3 and (b) \tilde{K}_C/q , where \tilde{K}_C is the spring constant between

blocks. Both interactions are zero outside the square interaction region. For case (a), Eq. (4) becomes

$$\sigma_i(t) = -K_L \phi_i(t) + \bar{K}_C \sum_j \frac{[\phi_j(t) - \phi_i(t)]}{|\vec{i} - \vec{j}|^3} \quad [\text{case (a)}], \quad (8)$$

where $|\vec{i} - \vec{j}|$ is the lattice distance between cells i and j . For case (b), Eq. (4) becomes

$$\sigma_i(t) = -K_L \phi_i(t) + \frac{\bar{K}_C}{q} \sum_j [\phi_j(t) - \phi_i(t)] \quad [\text{case (b)}]. \quad (9)$$

If we compare Eq. (9) to Eq. (4), we see that $K_C = \bar{K}_C/q$ for case (b), which means that $K = K_L + \bar{K}_C$ in Eq. (6) for every block i independently of q . In contrast, for case (a) in Eq. (6), $K = K_L + \bar{K}_C \sum_j |\vec{i} - \vec{j}|^{-3}$, which depends on q .

We can make the algorithm more efficient by eliminating $\phi_i(t)$ from the RJB equations. If we substitute Eq. (3) into Eqs. (8) or (9) and then into Eq. (5), we obtain

$$\sigma_i(t) = nK_L V \Delta T + \sum_j T_{ij} U_j(t), \quad (10)$$

$$U_j(t+1) = U_j(t) + J[\sigma_j(t)] \Theta[\sigma_j(t) - \sigma_{F,j}]. \quad (11)$$

For case (a), $T_{ij} = \bar{K}_C |\vec{i} - \vec{j}|^{-3}$ for $i \neq j$ and $T_{ii} = -K_L - \bar{K}_C \sum_j |\vec{i} - \vec{j}|^{-3}$. For case (b), $T_{ij} = \bar{K}_C/q$ for $i \neq j$ and $T_{ii} = -K_L - \bar{K}_C$. If we multiply Eq. (11) by T_{ij} and sum over j using Eq. (10), we can write

$$\sigma_i(t+1) = \sigma_i(t) + \sum_j T_{ij} J[\sigma_j(t)] \Theta[\sigma_j(t) - \sigma_{F,j}], \quad (12)$$

where the sum over j includes block i and its q neighbors. This equation evolves the stress during the rupture time. The modified algorithm becomes:

(1) Choose the value of $\sigma_{F,i}$ in the same way as for the nearest-neighbor algorithm, and assign random $\sigma_i(0) \in [0, \sigma_{F,i}]$.

(2) Increase $\sigma_i(0)$ by $K_L V \Delta T$, where $\Delta T = 1$ and V are chosen as previously explained. Increment $n \rightarrow n+1$. Set $t = 1$.

(3) Compute $\sigma_i(t)$ using Eq. (12) for all blocks. Increment $t \rightarrow t+1$.

(4) Repeat step (3) until all $\sigma_i(t) < \sigma_{F,i}$.

(5) Measure the physical quantities of interest.

(6) Return to step (2) and continue this procedure for a predetermined number of times.

We explore the physics of the long-range model and the nearest-neighbor RJB model in the problems. For instance, increasing the spring constant \bar{K}_C between the blocks in the long-range model more tightly couples them to each other and decreases the stress dissipation per block failure [see Eq. (5)]. Consequently, more stress remains

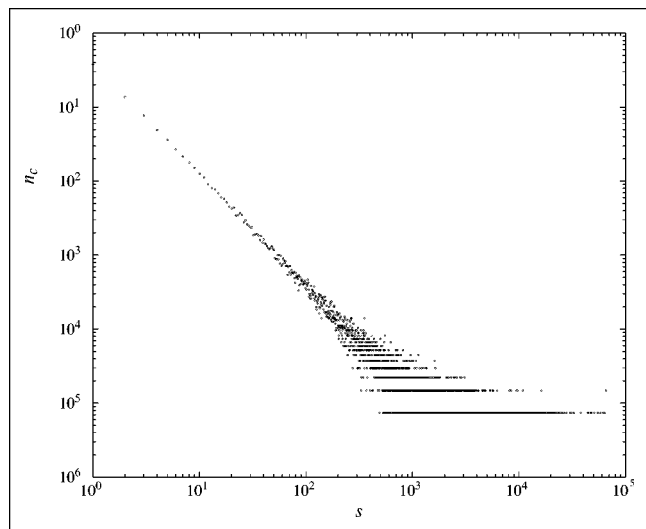


Figure 3. Log-log plot of the mean number of clusters $n_c(s)$ with s failed blocks for $L=256$ with the \bar{K}_C/q long-range interaction and periodic boundary conditions. The parameters are $R=16$ ($q=1088$), $\sigma_F=50$, $\sigma_R=0$, $\bar{K}_C=100$, $K_L=1$, and the zero-velocity limit using the stochastic jump function with $W=0.3$. The negative of the slope corresponds to $\tau=1.5$ in the interval $1 \leq s \leq 300$, implying that $b=0.75$.

available in the system to produce larger clusters. As we discuss in problem (5), the average cluster size increases linearly with \bar{K}_C , and the time to form the clusters increases as a power law with increasing \bar{K}_C . Figure 3 shows that cluster scaling for the long-range model differs from the nearest-neighbor model by having a smaller exponent. Therefore, clusters of a given size occur less frequently for the nearest-neighbor model in comparison to the long-range model.

Recent work¹⁹ demonstrates that the long-range interaction leads to a mean-field theory that displays stable, metastable, and unstable states. Most importantly, it predicts that earthquakes can form via nucleation. This prediction is interesting because nucleation may trigger real strike-slip earthquakes.²⁰ Although we still do not completely understand the causes of earthquakes, the study of long-range interaction models could point the way toward a deeper understanding.

Suggestions for further study

(1) Write a program to simulate the one-dimensional nearest-neighbor RJB model using the deterministic jump function and uniform values of $\sigma_{F,i}$. Consider linear dimensions $L = 64-256$. Although the choice of σ_F is arbitrary, we recommend choosing $\sigma_F = 50$. Set $\sigma_R = 0$. Choose either a small $V \approx \sigma_F/L^2$ to produce one initiator on average or use the zero-velocity-limit method. Take $K_L = 1$, and vary K_C from small values (< 1) to large values (> 10). Measure $n_c(s)$, the number of clusters of size s , and plot a histogram of n_c vs s . Does the s -dependence of $n_c(s)$ de-

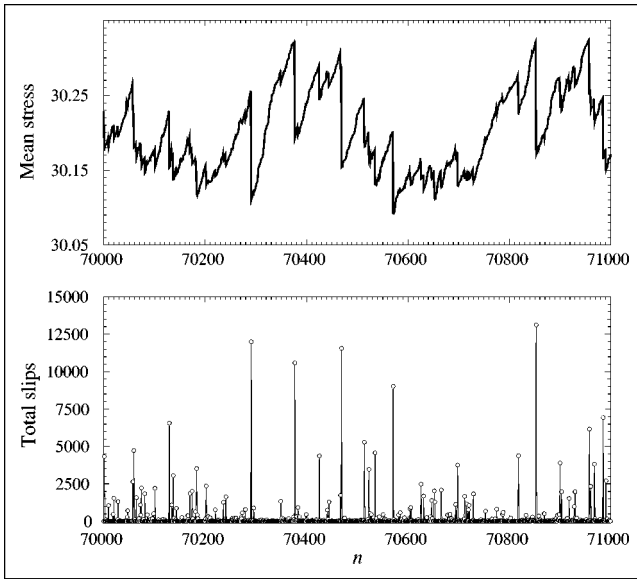


Figure 4. Plots of the mean stress and total slips versus plate update time n for $L=256$ and the r^{-3} long-range interaction truncated at $R=128$. Due to the choice of closed boundary conditions and the fact that $R=128$ encompasses a large portion of the system, $q=16129$ for the center blocks and $q=4288$ for the corner blocks, giving $\langle q \rangle \approx 10^4$. The parameters are $\sigma_F=50$, $\sigma_R=0$, $K_L=1$, $\bar{K}_C=25$, $\langle K \rangle \approx 250$, and the zero-velocity limit using the stochastic jump function with $W=0.3$.

pend on K_C ? We have found that $K_C < 1$ yields an exponential distribution, $K_C \sim O(1)$ produces a power-law distribution with an exponent that depends weakly on K_C , and $K_C \geq 10$ results in an excess of large quakes ($\approx L^2$) in comparison to the power-law distributions. These distributions are termed subcritical, critical, and supercritical scaling, respectively. Plot the time series of the mean stress versus the loader-plate update time n (see Fig. 4 for example). (The mean stress is obtained at a given time by averaging the magnitude of the stress over all blocks.) Observe the stick-slip pattern in the time series. The stick corresponds to increasing stress with only a few blocks moving, while the slip corresponds to a sudden drop in stress due to many blocks moving and releasing stress from the system. Does the average time between major slips occur more frequently or less often as K_C increases? What does this behavior say about the stress being dissipated and the interaction strength between the blocks?

(2) Use the stochastic jump function with different noise amplitudes in the program for problem (1). How does the inclusion of noise affect the cluster scaling and the time-series stick-slip patterns?

(3) Write a program to simulate the two-dimensional nearest-neighbor RJB model, repeating the measurements in problems (1) and (2). Do the two-dimensional results differ from the one-dimensional results?

(4) Write a program to simulate the long-range RJB model. Try both long-range stress tensors, cases (a) and (b), as previously defined. Values of R in the interval $2 \leq R \leq 8$

are adequate to observe effects different from those in the nearest-neighbor model. The capabilities of most personal computers and workstations will limit the interaction range to $R \approx 8$, which corresponds to $q = 288$ neighbors. For very-long-range interactions, the system size should be sufficiently large to allow earthquakes to grow beyond the size of the interaction region. For example, an $R=15$ system, which has $q=960$ blocks in an interaction region, should have $L \geq 256$. Use the stochastic jump function with $W \approx 0.3$. Measure $n_c(s)$ for different values of R . Take $K_L=1$, $\sigma_F=50$, and $\sigma_R=0$. Select values of \bar{K}_C to make K for the long-range interactions equal to K for the nearest-neighbor interactions in problems (2) and (3). How does the s -dependence of $n_c(s)$ compare to the case of nearest-neighbor interactions (see Fig. 3)? How does the cluster scaling of the long-range interaction in case (a) compare to that in case (b)? Is the time series of the mean stress for the long-range interaction model different than the time series for the nearest-neighbor model?

(5) Consider the long-range RJB model for various values of \bar{K}_C for a given value of R using either case (a) or (b) of the long-range interaction. Use the stochastic jump function with $W \approx 0.3$. Take $K_L=1$, $\sigma_F=50$, and $\sigma_R=0$. Measure the average equilibration time t_{equil} over which an earthquake occurs or a cluster forms. The equilibration time is the time required for the system to relax so that the stress on all blocks is below σ_F . To do this measurement, record the number of rupture time steps per plate update; then compute the time average of this quantity over many plate updates. Also measure the time-average cluster size \bar{s} , which is made by keeping track of the cluster size per plate update and then computing its average over many plate updates. Plot these quantities versus \bar{K}_C . What type of relationship is obtained? These plots should display a power law up to the value of \bar{K}_C that corresponds to supercritical scaling, as discussed above. Mean-field theory²¹ predicts that $t_{\text{equil}} \sim \bar{K}_C^{1/2}$ and $\bar{s} \sim \bar{K}_C$. Because the suggested interaction ranges are far from the mean-field limit, these scaling exponents will not be found exactly, but will approach their mean-field values as the interaction range R increases. The increased time to form an earthquake as \bar{K}_C approaches a critical value illustrates the phenomenon of critical slowing down,²² which is observed in many condensed-matter systems near a critical point.

(6) Examine the structure of the earthquake clusters. Are they fractal? If so, what is the fractal dimension? Do large clusters have holes in their interiors or perimeters or both? Or are these clusters dense filled-in objects? Do these structures depend on the system parameters? In particular, does the nearest-neighbor interaction produce different structures than the long-range interaction?

(7) Investigate the spatial and temporal rupture patterns. Several real strike-slip faults exhibit space-time clustering of events in which similar large-magnitude earthquakes tend to occur close to each other in space and time.

Then for a long duration, few large earthquakes will occur until another temporal grouping of large events. Time-series plots can display this temporal clustering. For instance, the plot of the total slips in Fig. 4 shows that intermediate-sized events ($\approx 10^3$ to 7×10^3 slips) occur in temporal clusters, whereas larger events are typically surrounded by quiescent periods. In addition to analyzing the time series for the temporal behavior of earthquakes, plot the spatial pattern of large events during a time sequence. Do these large events occupy similar sites? Are they adjacent to each other or are they separate? How do these spatial patterns evolve?

Acknowledgments

Two of the authors (C.D.F. and W.K.) received support from DOE Grant No. DE-FG02-95ER14498, and one author (J.B.R.) received support from DOE Grant No. DE-FG03-95ER14499. The authors thank Jonathan Goldstein for his questions and comments on the RJB model and the editors, Harvey Gould and Jan Tobochnik, for their helpful suggestions.

From the editors. Please consider submitting a manuscript to the Computer Simulations column. We also invite your comments and suggestions for future columns. Of particular interest are columns such as the present one that show students how to apply their knowledge of basic physics to model realistic problems of current interest. We also are interested in columns that illustrate how to use simple interactive graphics embedded in Fortran 90, C/C++, and Java simulation programs. For further information on submitting a manuscript, visit <http://physics.clarku.edu/cip/cip.html>.

References

1. B. A. Bolt, *Earthquakes* (W. H. Freeman and Company, San Francisco, 1993).
2. C. H. Scholz, *The Mechanics of Earthquakes and Faulting* (Cambridge University Press, Cambridge, 1990).
3. J. F. Pacheco, C. H. Scholz, and L. R. Sykes, *Nature* (London) **355**, 71 (1992).
4. H. F. Reid, *The California Earthquake of April 18, 1906, Report of the State Earthquake Commission* (Carnegie Institution, Washington, D.C., 1910).
5. B. Gutenberg and C. F. Richter, *Seismicity of the Earth and Associated Phenomena*, 2nd edition (Princeton University Press, Princeton, 1954).
6. R. Burridge and L. Knopoff, *Bull. Seismol. Soc. Am.* **57**, 341 (1967).
7. J. M. Carlson, J. S. Langer, and B. E. Shaw, *Rev. Mod. Phys.* **66**, 657 (1994).
8. J. B. Rundle and D. D. Jackson, *Bull. Seismol. Soc. Am.* **67**, 1363 (1977); J. B. Rundle and S. R. Brown, *J. Stat. Phys.* **65**, 403 (1991).
9. Z. Olami, H. J. S. Feder, and K. Christensen, *Phys. Rev. Lett.* **68**, 1244 (1992).
10. H. Kanamori and D. L. Anderson, *Bull. Seismol. Soc. Am.* **65**, 1073 (1975).
11. J. B. Rundle, W. Klein, and S. Gross, in *Reduction and Predictability of Natural Disasters*, edited by J. B. Rundle, D. L. Turcotte, and W. Klein (Addison-Wesley, Reading, MA, 1996), pp. 167–203.
12. H. Nakanishi, *Phys. Rev. A* **41**, 7086 (1990).
13. P. Grassberger, *Phys. Rev. E* **49**, 2436 (1994).
14. J. B. Rundle, W. Klein, S. Gross, and C. D. Ferguson, *Phys. Rev. E* **56**, 293 (1997).
15. J. A. Steketee, *Can. J. Phys.* **36**, 192 (1958).
16. D. P. Hill, P. A. Reasenberg, A. Michael, W. J. Arabaz, G. Beroza, D. Brumbaugh, J. N. Brune, R. Castro, S. Davis, D. dePolo, W. L. Ellsworth, J. Gomberg, S. Harmsen, L. House, S. M. Jackson, M. J. S. Johnston, L. Jones, R. Keller, S. Malone, L. Munguia, S. Nava, J. C. Pechmann, A. Sanford, R. W. Simpson, R. B. Smith, M. Stark, M. Stickney, A. Vidal, S. Walter, V. Wong, and J. Zollweg, *Nature* (London) **260**, 1617 (1993).
17. J. B. Rundle and W. Klein, *Nonlinear Processes Geophys.* **2**, 61 (1995).
18. D. W. Heermann and W. Klein, *Phys. Rev. B* **27**, 1732 (1983); D. W. Heermann, W. Klein, and D. Stauffer, *Phys. Rev. Lett.* **49**, 1262 (1982); W. Klein and C. Unger, *Phys. Rev. B* **28**, 445 (1983); T. S. Ray and W. Klein, *J. Stat. Phys.* **61**, 891 (1990); L. Monette and W. Klein, *Phys. Rev. Lett.* **68**, 2336 (1992); N. Gross, W. Klein, and K. Ludwig, *Phys. Rev. Lett.* **73**, 2639 (1994).
19. W. Klein, J. B. Rundle, and C. D. Ferguson, *Phys. Rev. Lett.* **78**, 3793 (1997).
20. W. L. Ellsworth and G. C. Beroza, *Science* **268**, 861 (1995).
21. C. D. Ferguson, W. Klein, and J. B. Rundle (to be published).
22. See, for example, H. Gould and J. Tobochnik, *Comput. Phys.* **3**(4) (1989), for a discussion of the computational issues involving critical slowing down in various condensed-matter systems.